2015

Smoking accelerates pancreatic cancer progression by promoting differentiation of MDSCs and inducing HB-EGF expression in macrophages

S. Kumar
University of Nebraska Medical Center

M. P. Torres
University of Nebraska Medical Center

S. Kaur
University of Nebraska Medical Center

S. Rachagani
University of Nebraska Medical Center

S. Joshi
University of Nebraska Medical Center

Recommended Citation

Kumar, S., Torres, M., Kaur, S. et al. Smoking accelerates pancreatic cancer progression by promoting differentiation of MDSCs and inducing HB-EGF expression in macrophages. Oncogene 34, 2052–2060 (2015). https://doi.org/10.1038/onc.2014.154

HHS Public Access

Author manuscript

Oncogene. Author manuscript; available in PMC 2015 October 16.

Published in final edited form as:

Oncogene. 2015 April 16; 34(16): 2052–2060. doi:10.1038/onc.2014.154.

Smoking accelerates pancreatic cancer progression by promoting differentiation of MDSCs and inducing HB-EGF expression in macrophages

S Kumar[1,9], **MP Torres**[1,2,9], **S Kaur**[1], **S Rachagani**[1], **S Joshi**[1], **SL Johansson**[3], **N Momi**[1], **MJ Baine**[1], **CE Gilling**[4], **LM Smith**[5], **TA Wyatt**[6], **M Jain**[1,7], **SS Joshi**[8], and **SK Batra**[1,2,7]

[1]Department of Biochemistry and Molecular Biology, University of Nebraska Medical Center, Omaha, NE, USA

[2]Eppley Institute for Research in Cancer and Allied Diseases, University of Nebraska Medical Center, Omaha, NE, USA

[3]Department of Pathology and Microbiology, University of Nebraska Medical Center, Omaha, NE, USA

[4]Department of Biology, University of Nebraska at Omaha, Omaha, NE, USA

[5]Department of Biostatistics, University of Nebraska Medical Center, Omaha, NE, USA

[6]Division of Pulmonary, Critical Care, Sleep & Allergy, University of Nebraska Medical Center, Omaha, NE, USA

[7]Fred and Pamela Buffett Cancer Center, University of Nebraska Medical center, Omaha, NE, USA

[8]Department of Genetics, Cell Biology and Anatomy, University of Nebraska Medical Center, Omaha, NE, USA

Abstract

Smoking is an established risk factor for pancreatic cancer (PC), but late diagnosis limits the evaluation of its mechanistic role in the progression of PC. We used a well-established genetically engineered mouse model (LSL-K-ras^{G12D}) of PC to elucidate the role of smoking during initiation and development of pancreatic intraepithelial neoplasia (PanIN). The 10-week-old floxed mice (K-ras^{G12D}; Pdx-1cre) and their control unfloxed (LSL-K-ras^{G12D}) littermates were exposed to cigarette smoke (total suspended particles: 150 mg/m^3) for 20 weeks. Smoke exposure significantly accelerated the development of PanIN lesions in the floxed mice, which correlated with tenfold increase in the expression of cytokeratin19. The systemic accumulation of myeloid-derived suppressor cells (MDSCs) decreased significantly in floxed mice compared with unfloxed

Correspondence: Dr SK Batra, Department of Biochemistry and Molecular Biology, Eppley Institute for Research in Cancer and Allied Diseases, University of Nebraska Medical Center, Omaha, NE 68198-5870, USA. sbatra@unmc.edu.

[9]These authors contributed equally to this work.

CONFLICT OF INTEREST

The authors declare no conflict of interest.

Supplementary Information accompanies this paper on the Oncogene website (http://www.nature.com/onc)

controls ($P<0.01$) after the smoke exposure with the concurrent increase in the macrophage ($P<0.05$) and dendritic cell (DCs) ($P<0.01$) population. Further, smoking-induced inflammation (IFN-γ, CXCL2; $P<0.05$) was accompanied by enhanced activation of pancreatic stellate cells and elevated levels of serum retinoic acid-binding protein 4, indicating increased bioavailability of retinoic acid which contributes to differentiation of MDSCs to tumor-associated macrophages (TAMs) and DCs. TAMs predominantly contribute to the increased expression of heparin-binding epidermal growth factor-like growth factor (EGFR ligand) in pre-neoplastic lesions in smoke-exposed floxed mice that facilitate acinar-to-ductal metaplasia (ADM). Further, smoke exposure also resulted in partial suppression of the immune system early during PC progression. Overall, the present study provides a novel mechanism of smoking-induced increase in ADM in the presence of constitutively active K-ras mutation.

INTRODUCTION

Pancreatic cancer (PC) is one of the most lethal malignancies with an overall 5-year survival rate of 6%.[1,2] One of the main reasons for its poor prognosis is that PC patients remain asymptomatic until the disease progresses to advanced stages. Mutations resulting in the constitutive activation of the K-ras gene are present in 90% of pancreatic tumors and are considered to be a critical initiating event in PC pathology.[3] However, the K-ras mutation alone is not sufficient to develop aggressive PC and requires the loss or mutations in other tumor suppressor genes. Furthermore, the role of tumor microenvironment (TME) is increasingly being appreciated as an essential component required for the progression of the cancer. Components of TME viz, cancer-associated fibroblasts, endothelial cells and most importantly, the immune system have a critical role in the progression of the cancer. Myeloid-derived suppressor cells (MDSCs) have recently been suggested to have a key role in tumor-derived immune suppression.[4–6] These immature cells of myeloid origin appear in the peripheral circulation at pre-neoplastic stages, significantly suppress T-cell activity, and promote the development of T regulatory cells,[7] thereby helping tumors to evade the immune surveillance.

In addition to mutations and TME, studies have shown that obesity[8] and smoking[9,10] are the two major epidemiologically established preventable risk factors for PC. Smoking is the leading cause of mortality and morbidity worldwide and is a major health issue due to its epidemic proportion.[11,12] Cigarette smoke contains a complex mixture of over 4000 compounds having carcinogenic effects,[12,13] which influences all aspects of tumor biology including initiation, progression and metastasis through mutations,[14] inflammation[15] and immunosuppression.[11,12,16] Nevertheless, due to the late diagnosis of PC, the evaluation of these risk factors at early stages of PC progression is limited.

In the present study, we investigated the role of smoking at early stages of PC progression in a genetically engineered mouse model (that is, K-ras^{G12D}; Pdx-1cre),[17,18] which endogenously expresses an oncogenic K-ras allele in the pancreas and recapitulates the entire spectrum of human PC from pancreatic intraepithelial neoplasia (PanIN) lesions to invasive ductal carcinoma. K-ras^{G12D}; Pdx-1cre mice were exposed to cigarette smoke for 20 weeks after the emergence of PanIN lesions (that is, 10 weeks of age, PanIN-1).[17]

Overall, smoking resulted in a significant increase in low-grade PanIN formation in K-ras^{G12D}; Pdx-1cre mice. There was reduction in MDSCs after smoke exposure, which was partially attributed to the presence of alltrans retinoic acid (ATRA) secreted by activated pancreatic stellate cells (PSCs). ATRA alone or in combination with cytokines potentially leads to the maturation of MDSCs to tumor-associated macrophages (TAMs) and dendritic cells (DCs). Our study further suggests that smoke exposure increased the expression of heparin-binding epidermal growth factor-like growth factor (HB-EGF) in TAMs in TME, which in conjunction with constitutively active K-ras mutation has been shown to accelerate the pre-neoplastic PC progression.

RESULTS

The cigarette smoke exposure regimen followed by us resulted in circulating cotinine levels of 125.0 ± 15.6 ng/ml. Lung lavage analysis demonstrated elevated lung chemokines and neutrophil numbers (data not shown), which was in agreement with previous studies.[19]

Smoking aggravates PanIN lesion formation

All the floxed mice developed PanINs by 30 weeks of age with complete penetrance, whereas the pancreas of unfloxed mice were unremarkable (Figure 1a). Smoking significantly accelerated the PanIN (PanIN-1 and -2) formation in the floxed mice as compared with sham controls (Figures 1a and b). There was a significant increase in the number of the PanINs per higher-power field ($P = 0.0064$). Real time reverse transcription PCR analysis from the RNA isolated from pancreas of smoke-exposed floxed mice showed an tenfold increase in the expression of CK19 (ductal marker) with concurrent decrease in the amylase expression levels (acinar marker) (Figure 1c). The accelerated formation of PanIN lesions in response to smoking and the switching of markers from acinar to ductal type suggest enhanced acinar-to-ductal metaplasia (ADM) and experimentally support the epidemiological data of smoking being a risk factor for PC.

Smoking modulates the mobilization and accumulation of MDSCs

MDSCs consisting of two subsets (monocytic (CD11b+Ly6C^{hi}-Ly6G^{-}) and the granulocytic (CD11b+Ly6C^{low}Ly6G^{high}) fractions) (Figure 2a) appear early during pre-neoplastic conditions and contribute to tumor progression and tumor-associated immune suppression. The granulocytic fraction was the major subset that accumulated in the peripheral circulation, spleen ($P<0.001$) and bone marrow in the floxed mice (Figures 2b and c). Likewise, there was a significant accumulation of the monocytic ($P= 0.002$) and granulocytic ($P = 0.002$) fractions of MDSCs in the liver, which is the primary site for the PC metastasis (Supplementary Figures 2A and B). Conflicting to our expectation, MDSCs (granulocytic subset preferentially) decreased in the peripheral circulation (Figure 2b), bone marrow ($P<0.001$) and spleen ($P = 0.001$) (Figure 2c) of floxed mice after smoke exposure compared with sham controls. Validating our data, *in vitro* treatment of the splenocytes isolated from 30-week-old floxed mice with conditioned media from untreated or smoke lysate (SL)-treated KCT 961 cells (cell line derived from mouse tumor) significantly decreased the granulocytic population ($P<0.01$) (Figure 2d).

Smoking leads to activation of PSC and elevated levels of retinoic acid in circulation

The decrease in MDSCs following smoke exposure in floxed mice could either be due to their maturation or apoptosis and previous studies have characterized the role of ATRA and cytokines in MDSCs maturation.[20–22] One potential source of ATRA in TME is PSCs,[23–26] which on activation under inflammatory conditions secrete ATRA and express myofibroblast markers (α-SMA).[27] Indeed, smoking resulted in the increased activation of PSCs in floxed mice (composite score 5.0) compared with sham controls (composite score 3.3), as assessed by α-SMA staining (Figure 3a). ATRA in the serum is transported by retinoic acid-binding protein 4,[28] which is also considered as a surrogate marker for the circulating ATRA levels. There was a significant increase in the retinoic acid-binding protein 4 levels ($P<0.05$) in the sera of smoked animals compared with sham controls in both unfloxed and floxed mice, suggesting the presence of higher levels of ATRA in circulation (Figure 3b, Supplementary Figure 3). The impact of smoking on the PSCs was evaluated *in vitro* by treating PSC lines derived from pancreas (imPSCc2) with SL alone and the conditioned media from untreated or SL-treated KCT 961 cells. There was a significant increase in Ki-67 staining (nuclear localization) and higher expression of α-SMA in imPSCc2 cells after treatment with SL as well as with conditioned media from untreated and SL-treated cancer cells, demonstrating the role of smoking on greater activation and proliferation of PSCs (Figures 3c and d).

Cigarette smoke modulates the expression of cytokines and promotes inflammation

The levels of cytokines involved in the mobilization, maturation and activation of MDSCs were estimated in the sera of smoke-exposed and sham mice (Figure 4, Supplementary Figures 4A and F). The levels of cytokines, such as granulocyte-macrophage colony-stimulating factor (GM-CSF), interleukin (IL)-1β and IL-2, were higher in floxed mice in comparison to unfloxed group but their levels reduced after smoke exposure in floxed mice, consistent with the reduction in MDSCs (Supplementary Figures 4A and C). In addition, we observed increased levels of IL-12p40 and IL-6 (DCs specific cytokines) in smoked group compared with sham controls in floxed mice (Figure 4a). No significant differences were observed in the levels of other cytokines, such as G-CSF, M-CSF, IL-10, IL-13, TGF-β or tumor necrosis factor alpha (TNF-α) and macrophage inflammatory protein 1 alpha (MIP-1α), across the different experimental groups. The levels of inflammatory markers including *IFN-γ*, *CXCL1* and *CXCL2* increased in the pancreas of smoke-exposed floxed mice (~ twofold) compared with sham controls (Figure 4b). In agreement with these results, there was an increase in the overall degree of inflammation in the pancreas after smoke exposure (inflammatory score 1–2) compared with sham controls (inflammatory score 0–2) (Supplementary Table 4) as indicated by increased presence of mononucleated cells.

Increased accumulation of macrophages and DCs after smoke exposure

The decrease in the MDSCs was attributed to their differentiation to macrophages and DCs in response to factors including ATRA.[22,29–31] This premise was strengthened by a significant increase (*$P<0.05$) in the number of TAMs (F4/80-positive cells) in the pancreas of floxed mice after smoke exposure (average area 1.3%, average intensity 1.6, $n = 5$) compared with sham controls (average area <1%, average intensity 1.3, $n = 5$) (Figure 5a).

The median number of infiltrating macrophages was significantly higher in smoke-exposed (average count of 50/field) mice as compared with sham controls (average count of 20/field), as well as there was an increase in the DC population ($CD80^{H}CD86^{H}$) in liver and spleen ($P<0.001$) (Figures 5b and c). However, there was no significant difference in the DC population in pancreas of sham and smoke-exposed groups.

Smoking upregulates HB-EGF expression in macrophages

The presence of TAMs correlates with aggressive phenotype and poor prognosis in solid tumors.[32] Further, in PC, aberrant overexpression of EGFR ligands, especially HB-EGF by TAMs, has been associated with ADM and early appearance of the PanIN lesions in K-ras^{G12D} (KC) mice.[33,34] EGFR signaling is in fact essential in promoting K-ras-oncogene-driven progression of PC, especially in presence of wild-type p53.[33,35] In parallel to this, we have observed sevenfold increase in the expression of HB-EGF in the pancreas of the floxed mice following smoke exposure (Figure 6a), and immunofluorescence analysis using F4/80 and HB-EGF antibodies in floxed mice demonstrated that macrophages were indeed the predominant source of the HB-EGF in PanIN-associated stroma following smoke exposure (Figures 6b and c). *In vitro* treatment of mouse macrophage cell line RAW 264.7 with conditioned media derived from SL-treated KCT 961 PC cell line also resulted in 2.8-fold increase in HB-EGF at transcription level (Figure 6d) and similarly, there was increase in protein levels of HB-EGF as well (Supplementary Figure 5).

Smoking partially suppressed the immune response at initial stages of PC progression

To confirm the functional status of immune system, peripheral blood mononucleated cells and splenocytes isolated from sham and smoke-exposed mice were stimulated with the T/B-cell mitogens concanavalin A (Con A), phytohemagglutinin (PHA) and pokeweed mitogen (PW). Lymphocytes from the blood of unfloxed smoke-exposed mice proliferated at significantly higher rates in response to both PHA and PW when compared with sham controls (Figure 7a); however, the lymphocyte proliferation potential from peripheral circulation reduced after the smoke exposure along with the decrease in the $CD3^{+}TCR^{+}$ population in peripheral circulation (Supplementary Figure 6), suggesting the partial suppression of the immune system in the mice with pre-neoplastic lesions in response to smoke exposure (Figure 7a). On the other hand, splenocytes proliferated at comparable levels to mitogen stimulation even after the smoke exposure in unfloxed and floxed mice (Figure 7b). This smoking-induced immune suppression further helped tumor to accelerate faster.

DISCUSSION

Epidemiological studies have recognized smoking as a significant risk factor for PC[9,10] and the experimental evidence indicates that smoke exposure modulates macrophage, DC and T-cell functions in vitro.[16,36,37] A previous study investigating the immune response to PC in K-ras^{G12D} mouse model demonstrated infiltration of MDSCs and regulatory T cells during the development of PanIN lesions.[38] The increased frequency of PanIN lesion formation in the pancreas of floxed animals after smoking as compared with the sham controls in the present study establish a direct association between smoking and higher risk of PC

development in individuals harboring constitutively active *K-ras* mutation in the pancreas. The increased expression of the epithelial marker, CK19 and α-SMA suggests that chronic inflammation induced by smoking facilitates the ADM and accumulation of fibrotic stroma in *K-ras*^{G12D}; Pdx-1cre mice respectively, much similar to BK5.COX2 chronic pancreatitis transgenic mice, which develops pancreatic ductal adenocarcinoma by 6–8 months of age.[39]

The presence of PanIN lesions leads to the mobilization and accumulation of MDSCs in different organs. Serum cytokine analysis revealed higher levels of factors involved in the recruitment and maturation of MDSCs, such as GM-CSF[40,41] and IL-1β, in floxed mice compared with unfloxed mice. The decrease in the MDSCs (CD11b+ Gr1+ (Ly6C, Ly6G)) after smoke exposure in our study was unexpected; however, the concurrent increase in the DC and macrophage population suggested maturation and/or apoptosis of MDSCs. A previous study by Kusmartsev et al.[21] has demonstrated that immature cells of myeloid origin ($CD11b^+$ $Gr\text{-}1^+$) differentiate into macrophage (F4/80) and DC ($CD11c^+CD86^+$) populations in response to ATRA both under in vitro and in vivo conditions. ATRA is also known to induce differentiation of acute promyelocytic leukemia[42] and hematopoietic progenitor cell.[43] Further, vitamin A deficiency in mice leads to the expansion of immature myeloid fraction, highlighting the importance of ATRA in the maturation of myeloid lineage.[44]

The increased level of ATRA after the smoke exposure in our study strengthens our assumption that smoking resulted in exaggerated inflammatory response leading to enhanced activation of the PSCs. The quiescent stellate cells store retinoic acid in fat droplets as retinoid and upon activation by inflammatory stimuli secrete their retinoid store as ATRA[23–25,45] and start expressing α-SMA.[27] The increased expression of α-SMA in the pancreas after smoke exposure suggests higher activation status of PSCs, which was also validated in vitro by significant increase in Ki-67 expression and nuclear localization in PSCs (imPSCc2) after treatment with SL and conditioned media from SL-treated cancer cell line (KCT 961). The increased activation of PSCs in response to smoke exposure was corroborated by previous work documenting higher levels of pancreatic fibrosis in smokers compared with never smokers.[46] The increased levels of IL-12p40 cytokine secreted by DCs matured explicitly in response to ATRA, suggesting the involvement of ATRA in smoking-mediated immune modulation.[47]

We believe that increase in TAMs due to differentiation of MDSCs or their higher infiltration accelerates the PanIN formation. Previous reports have established that increased macrophage accumulation in early pre-neoplastic lesions in pancreas accelerates ADM and phenotypic changes associated with PC initiation.[33,34] These PanIN-associated macrophages are predominant source of cytokines and the EGFR ligands in multiple cancers.[33,48] EGFR-mediated signaling has been demonstrated to be essential and acts synergistically with activated K-ras to drive PC oncogenesis[35] involving multiple signaling pathways. Further, studies have specifically demonstrated that TAMs are the primary source of HB-EGF (EGFR ligand) in the microenvironment as compared with classically activated macrophages.[49] In pancreas, HB-EGF has been demonstrated to promote ADM in the presence of K-ras mutation and promotes the development of PanINs and PDAC *in vivo*.[33] Therefore, higher expression of HB-EGF in the pancreas of floxed mice after smoke

exposure mechanistically explains the increase in PanIN formation and faster progression of PC. Furthermore, the present study has also demonstrated that TAMs are the principal source of HB-EGF in pre-neoplastic microenvironment, as reported previously. In addition to EGFR-mediated signaling, the impairment of immune system due to persistent smoke exposure demonstrated by us and others[12,16,36] also assisted in the faster progression of the PC.

Taken together, present study provides a novel mechanism for smoking-induced acceleration of the PC progression (Figure 7c) through differentiation of immature myeloid cells into tumor-promoting macrophage population (in response to ATRA and cytokines), expressing higher levels of HB-EGF in TME.[33] However, to fully understand the role of TAM-derived HB-EGF in smoking-induced PanIN progression in KC mice, further studies involving macrophage-targeted conditional knockout of HB-EGF need to be undertaken. In addition, it is important to emphasize that chronic inflammation and progression of cancer may tip the scale toward the expansion of the MDSC compartment later during PC progression.

MATERIALS AND METHODS

Smoke exposure

All animal experiments were reviewed and approved by the University of Nebraska Medical Center Institutional Animal Care and Use Committee (IACUC). The animals (LSL-K-ras^{G12D} and K-ras^{G12D}; Pdx-1cre referred as unfloxed and floxed, respectively) were exposed to cigarette (University of Kentucky Reference Cigarette, 3R4F, Lexington, KY, USA) smoke (Teague TE-10C, Davis, CA, USA) for 20 weeks, 3 h twice a day (150 mg total suspended particles/m^3) starting at 10 weeks of age when floxed mice start developing low-grade PanIN lesions.[17] Sham animals were used as controls (Supplementary Table 1).

Real time PCR analysis

Total RNA from pancreas and RAW 264.7 cells was isolated using the mirVana miRNA kit (Applied Biosystems, Austin, TX, USA) and Qiagen RNeasy Kits (Qiagen, Valencia, CA, USA), respectively. RNA (1 μg) was reverse transcribed with random hexamer oligo (500 μg/ml) as previously described.[50] Subsequently, for real time PCR analysis, 10 ng of complementary DNA was amplified using the Light Cycler 480 SYBR green I master mix (Roche Diagnostics, Indianapolis, IN, USA) in the Light Cycler 480II (Roche Diagnostics). The amplification was done in a two-step cyclic process (95 °C for 5 min, followed by 45 cycles of 95 °C for 10 s, 60 °C for 10 s and 72 °C for 10 s). The expression of various genes was profiled using gene-specific primers (Supplementary Table 2) and the relative expression was calculated using $2^{\Delta\Delta}C_T$ method. Statistical comparisons of two groups were made using Student's *t*-test and $P<0.05$ was considered statistically significant.

Cellularity analysis

Cells from bone marrow were isolated by flushing the femur 3–4 times with RPMI media supplemented with 10% fetal bovine serum and penicillin/streptomycin. Single cell suspension from tissues (n =6) was prepared by repetitive passaging through 25 gauge needles and the cells from blood were analyzed after red blood cell lysis using RBC Lysis

Buffer (BD Bioscience, San Jose, CA, USA). Cells from pancreas and blood from each experimental group were pooled ($n = 6$) before staining. The cells were stained with the indicated antibody cocktail for 1 h on ice and fixed in 4% paraformaldehyde in phosphate-buffered saline (PBS). The stained cells were analyzed on a BD Bioscience LSRII flow cytometer (BD Bioscience). The mouse-specific antibodies and isotype controls used for flow cytometry were purchased from BD Bioscience and eBioscience (San Diego, CA, USA) (Supplementary Table 3). The gating strategy is described in Supplementary Figure 1.

Western blot analysis

Western blot analysis was performed as previously described.[51] Briefly, serum samples were mixed with Laemmli buffer and resolved on 10% SDS–PAGE. Proteins were transferred to polyvinylidene difluoride membrane and incubated overnight with RBP4 antibody (2947-1, Epitomics, Burlingame, CA, USA) and HB-EGF (sc1414, Santa Cruz Biotechnology, Santa Cruz, TX, USA) after blocking with 5% skim milk. The blot was washed three times with PBST (0.1% Tween 20) and incubated with horseradish peroxidase-conjugated secondary antibody (Thermo Scientific, Rockford, IL, USA) for 1 h at room temperature. Membrane was washed with PBST and the proteins were visualized by enhanced chemiluminescent reagent (Thermo Scientific). Protein bands for RBP4 were quantified using ImageJ software (NIH, Bethesda, MD, USA), and *P*-values were calculated using Student's *t*-test of replicate values and values <0.05 were considered to be statistically significant. Nonspecific protein band in the blot was used for loading control and normalization.

Cytokine assay

For the analysis of various cytokines, blood was allowed to clot and centrifuged at 1000 g for 30 min. The serum levels of pro-inflammatory cytokines, chemokines and growth factors (G-CSF, GM-CSF, IFN-γ, IL-10, IL-12p70, IL-13, IL-1beta, IL-2, IL-4, IL-6, M-CSF/CSF1) were assessed utilizing a customized Luminex-based multiplex Procarta Cytokine Assay Kit (Multimetrix, Heidelberg, Germany). Standard curves were prepared from standards provided with the kit and serially ($\log_4$) diluted from 20 ng/ml to 1.2 pg/ml.

In vitro lymphocyte stimulation assay

Peripheral blood mononucleated cells and splenocytes were seeded, in triplicate in 96-well plates (2×10^5/well). The mitogens Con A, PHA at 2.5 μg/ml each and PW at 5 μg/ml final concentration were added to each well. After 72 h of incubation, 1 μCi of ^{3}H-thymidine (MP Biomedicals, Solon, OH, USA) was added to each well and plates were incubated for 18 h. Cells were collected onto glass fiber filter paper discs using a PHD Cell Harvester (Cambridge Technology Inc, Lexington, MA, USA). The dried filter discs were placed in scintillation counting vials containing scintillation fluid (ScintiVerse CTM Scintillation medium, Fisher Scientific, Pittsburg, PA, USA) and the counts per minute (c.p.m.) were recorded in a TRI-CARB 2100 TR Packard Liquid Scintillation Analyzer (PerkinElmer, Boston, MA, USA) and used to calculate stimulation index (c.p.m. of smoke exposed/c.p.m. of sham). Student's *t*-test of replicate values was used to calculate the corresponding *P*-values (<0.05 was considered to be statistically significant).

Immunohistochemistry analysis

Tissues (pancreas) from mice were collected and fixed in 10% formalin for 72 h and embedded in paraffin wax. Immunohistochemistry analysis was performed as described previously.[50] Briefly, glass slides containing 5-μm-thick tissue sections were baked overnight at 58 °C. After deparaffinization with xylene, tissues were rehydrated in decreasing concentrations of ethanol. Endogenous peroxidase activity was blocked by incubating tissues for 1 h with 3% H_2O_2:methanol solution. Antigens were retrieved by boiling sections in 0.5% citrate buffer for 15 min, blocked with 2.5% horse serum for 1 h and incubated with α-smooth muscle actin (α-SMA; ab18147, Abcam, Cambridge, MA, USA), murine F4/80 (123102, Biolegend, San Diego, CA, USA) and primary antibodies overnight at 4 °C. Slides were washed with PBS and incubated with horseradish peroxidase-conjugated secondary antibodies for 1 h, washed and developed for colorimetric detection by the 3.3′ diaminobenzidine kit (Vector laboratories, Burlingame, CA, USA). After counterstaining with hematoxylin, the tissues were dehydrated, dried and mounted with Permount (Cat. No. 17986-05, Fisher Scientific, Hatfield, PA, USA). The intensity of the staining was evaluated by pathologist. The composite score for α-SMA was calculated on the basis of intensity (scale of 0–3) and percentage positivity (0–100%). The TAM from sham and smoke-exposed animals (n = 5) were quantified by counting F4/80-positive cells from five independent fields per tissue section and the results were presented as the average count of five independent fields. Further, slides were evaluated by pathologist and the staining in tissues was evaluated on the basis of percentage average area (area occupied by macrophage staining/section) and intensity of staining (scale of 0–3).

Immunofluorescence analysis

Immunofluorescence analysis of pancreas after smoke exposure was performed on 5-μm-thick tissue sections mounted onto glass slides that were baked overnight at 58 °C. Tissues were deparaffinized with xylene, rehydrated in decreasing concentrations of ethanol and permeabilized for 30 min with methanol solution. Antigen retrieval was performed by boiling sections in 0.5% citrate buffer for 15 min, blocked with 2.5% horse serum for 1 h and incubated with murine F4/80 and HB-EGF (sc1414, Santa Cruz Biotechnology) primary antibodies overnight at 4 °C. Slides were washed with PBS and incubated with FITC-conjugated (A-629511, Invitrogen, Grand Island, NY, USA) and Alexa-Fluor-647 (A-21447, Invitrogen)-conjugated secondary antibodies for 1 h, washed three times and mounted with Vectashield containing 4′ 6′-diamidino-2-phenylindole (DAPI).

In vitro cell treatment with SL

The cigarette SL for in vitro experiments was prepared as described previously.[52] Briefly, two 3R4F cigarettes smoke was passed directly through 35 ml media in air-tight glass container at the rate of 1 puff (2 s duration) for 8 min, providing ~ 0.8 mg nicotine/cigarette. The splenocytes from the 30-week-old floxed mice were isolated and exposed for 48 h to either smoke lysate (1:100 in 10% RPMI) alone (SL) or to the conditioned media from cancer cell line (KCT 961, derived from K-ras^{G12D}, TP53^{R172H}; Pdx1-cre mouse pancreatic tumor, T) and cancer cell line treated with SL for 24 h (T+SL). The conditioned media were also used to treat PSCs and RAW 264.7 cells. After incubation, the splenocytes were

analyzed for the expression of indicated markers by flow cytometry analysis. Splenocytes were stained with the indicated antibody cocktail for 1h on ice, fixed in 4% paraformaldehyde and analyzed on BD Bioscience LSRII flow cytometer (BD Bioscience). PSCs (imPSCc2, kindly gifted by Dr Raul A Urrutia, Mayo Clinics)[53] seeded on glass coverslips were treated and stained with α-SMA and Ki-67 (ab66155, Abcam) primary antibodies for 1 h. Cells were washed three times with PBS and incubated with Alexa Fluor-488 (anti-mouse, A11001, Invitrogen) and Alexa Fluor-568 (anti-rabbit, A11011, Invitrogen) secondary antibodies for 1 h. Cells were again washed three times and mounted with Vectashield containing DAPI.

Statistical analysis

The Kruskal–Wallis test was used to compare the distribution of percent gated cells and cytokine analysis. If the overall test was statistically significant, pairwise comparisons between the groups were conducted and *P*-values were adjusted for multiple comparisons using the Bonferroni method. *P*-value <0.05 was considered statistically significant.

Supplementary Material

Refer to Web version on PubMed Central for supplementary material.

Acknowledgments

We are grateful to Dr Patrick C Swanson, Creighton University, Omaha, for suggestions. We appreciate the UNMC Cell Analysis Facility for analysis and graduate students and technician Erik Moore from Dr Batra's lab for help in sample preparation. This work was supported in part by the grant from National Institute of Health (R01CA78590, EDRN U01 CA111294, R01 CA133774, R01 CA131944, SPORE P50 CA127297, T32 CA009476, P20 GM103480, R21 CA156037 and U54 TMEN CA163120).

References

1. Braat H, Bruno M, Kuipers EJ, Peppelenbosch MP. Pancreatic cancer: promise for personalised medicine? Cancer Lett. 2012; 318:1–8. [PubMed: 22178657]
2. Siegel R, Naishadham D, Jemal A. Cancer statistics, 2012. CA Cancer J Clin. 2012; 62:10–29. [PubMed: 22237781]
3. Maitra A, Hruban RH. Pancreatic cancer. Annu Rev Pathol. 2008; 3:157–188. [PubMed: 18039136]
4. Gabrilovich DI, Nagaraj S. Myeloid-derived suppressor cells as regulators of the immune system. Nat Rev Immunol. 2009; 9:162–174. [PubMed: 19197294]
5. Toh B, Wang X, Keeble J, Sim WJ, Khoo K, Wong WC, et al. Mesenchymal transition and dissemination of cancer cells is driven by myeloid-derived suppressor cells infiltrating the primary tumor. PLoS Biol. 2011; 9:e1001162. [PubMed: 21980263]
6. Zhao F, Obermann S, von WR, Haile L, Manns MP, Korangy F, et al. Increase in frequency of myeloid-derived suppressor cells in mice with spontaneous pancreatic carcinoma. Immunology. 2009; 128:141–149. [PubMed: 19689743]
7. Huang B, Pan PY, Li Q, Sato AI, Levy DE, Bromberg J, et al. Gr-1+CD115+ immature myeloid suppressor cells mediate the development of tumor-induced T regulatory cells and T-cell anergy in tumor-bearing host. Cancer Res. 2006; 66:1123–1131. [PubMed: 16424049]
8. Bracci PM. Obesity and pancreatic cancer: overview of epidemiologic evidence and biologic mechanisms. Mol Carcinog. 2012; 51:53–63. [PubMed: 22162231]
9. Duell EJ, Holly EA, Bracci PM, Liu M, Wiencke JK, Kelsey KT. A population-based, case-control study of polymorphisms in carcinogen-metabolizing genes, smoking, and pancreatic adenocarcinoma risk. J Natl Cancer Inst. 2002; 94:297–306. [PubMed: 11854392]

10. Duell EJ. Epidemiology and potential mechanisms of tobacco smoking and heavy alcohol consumption in pancreatic cancer. Mol Carcinog. 2012; 51:40–52. [PubMed: 22162230]
11. Sopori M. Effects of cigarette smoke on the immune system. Nat Rev Immunol. 2002; 2:372–377. [PubMed: 12033743]
12. Sopori ML, Kozak W. Immunomodulatory effects of cigarette smoke. J Neuroimmunol. 1998; 83:148–156. [PubMed: 9610683]
13. Zeidel A, Beilin B, Yardeni I, Mayburd E, Smirnov G, Bessler H. Immune response in asymptomatic smokers. Acta Anaesthesiol Scand. 2002; 46:959–964. [PubMed: 12190796]
14. Blackford A, Parmigiani G, Kensler TW, Wolfgang C, Jones S, Zhang X, et al. Genetic mutations associated with cigarette smoking in pancreatic cancer. Cancer Res. 2009; 69:3681–3688. [PubMed: 19351817]
15. Malfertheiner P, Schutte K. Smoking–a trigger for chronic inflammation and cancer development in the pancreas. Am J Gastroenterol. 2006; 101:160–162. [PubMed: 16405549]
16. Nouri-Shirazi M, Guinet E. Evidence for the immunosuppressive role of nicotine on human dendritic cell functions. Immunology. 2003; 109:365–373. [PubMed: 12807482]
17. Hingorani SR, Petricoin EF, Maitra A, Rajapakse V, King C, Jacobetz MA, et al. Preinvasive and invasive ductal pancreatic cancer and its early detection in the mouse. Cancer Cell. 2003; 4:437–450. [PubMed: 14706336]
18. Hingorani SR, Wang L, Multani AS, Combs C, Deramaudt TB, Hruban RH, et al. Trp53R172H and KrasG12D cooperate to promote chromosomal instability and widely metastatic pancreatic ductal adenocarcinoma in mice. Cancer Cell. 2005; 7:469–483. [PubMed: 15894267]
19. Elliott MK, Sisson JH, West WW, Wyatt TA. Differential in vivo effects of whole cigarette smoke exposure versus cigarette smoke extract on mouse ciliated tracheal epithelium. Exp Lung Res. 2006; 32:99–118. [PubMed: 16754475]
20. Hengesbach LM, Hoag KA. Physiological concentrations of retinoic acid favor myeloid dendritic cell development over granulocyte development in cultures of bone marrow cells from mice. J Nutr. 2004; 134:2653–2659. [PubMed: 15465762]
21. Kusmartsev S, Cheng F, Yu B, Nefedova Y, Sotomayor E, Lush R, et al. All-trans-retinoic acid eliminates immature myeloid cells from tumor-bearing mice and improves the effect of vaccination. Cancer Res. 2003; 63:4441–4449. [PubMed: 12907617]
22. Nefedova Y, Fishman M, Sherman S, Wang X, Beg AA, Gabrilovich DI. Mechanism of all-trans retinoic acid effect on tumor-associated myeloid-derived suppressor cells. Cancer Res. 2007; 67:11021–11028. [PubMed: 18006848]
23. Apte MV, Haber PS, Applegate TL, Norton ID, McCaughan GW, Korsten MA, et al. Periacinar stellate shaped cells in rat pancreas: identification, isolation, and culture. Gut. 1998; 43:128–133. [PubMed: 9771417]
24. Bachem MG, Schneider E, Gross H, Weidenbach H, Schmid RM, Menke A, et al. Identification, culture, and characterization of pancreatic stellate cells in rats and humans. Gastroenterology. 1998; 115:421–432. [PubMed: 9679048]
25. McCarroll JA, Phillips PA, Santucci N, Pirola RC, Wilson JS, Apte MV. Vitamin A inhibits pancreatic stellate cell activation: implications for treatment of pancreatic fibrosis. Gut. 2006; 55:79–89. [PubMed: 16043492]
26. McCarroll JA, Phillips PA, Park S, Doherty E, Pirola RC, Wilson JS, et al. Pancreatic stellate cell activation by ethanol and acetaldehyde: is it mediated by the mitogen-activated protein kinase signaling pathway? Pancreas. 2003; 27:150–160. [PubMed: 12883264]
27. Habisch H, Zhou S, Siech M, Bachem MG. Interaction of stellate cells with pancreatic carcinoma cells. Cancers (Basel). 2010; 2:1661–1682. [PubMed: 24281180]
28. Hutchison SK, Harrison C, Stepto N, Meyer C, Teede HJ. Retinol-binding protein 4 and insulin resistance in polycystic ovary syndrome. Diabetes Care. 2008; 31:1427–1432. [PubMed: 18390799]
29. Manicassamy S, Pulendran B. Retinoic acid-dependent regulation of immune responses by dendritic cells and macrophages. Semin Immunol. 2009; 21:22–27. [PubMed: 18778953]

30. Mirza N, Fishman M, Fricke I, Dunn M, Neuger AM, Frost TJ, et al. All-trans-retinoic acid improves differentiation of myeloid cells and immune response in cancer patients. Cancer Res. 2006; 66:9299–9307. [PubMed: 16982775]
31. Ding Q, Jin T, Wang Z, Chen Y. Catalase potentiates retinoic acid-induced THP-1 monocyte differentiation into macrophage through inhibition of peroxisome proliferator-activated receptor gamma. J Leukoc Biol. 2007; 81:1568–1576. [PubMed: 17369494]
32. Zhang QW, Liu L, Gong CY, Shi HS, Zeng YH, Wang XZ, et al. Prognostic significance of tumor-associated macrophages in solid tumor: a meta-analysis of the literature. PLoS One. 2012; 7:e50946. [PubMed: 23284651]
33. Ray KC, Moss ME, Franklin JL, Weaver CJ, Higginbotham J, Song Y, et al. Heparin-binding epidermal growth factor-like growth factor eliminates constraints on activated Kras to promote rapid onset of pancreatic neoplasia. Oncogene. 2013; 33:823–831. [PubMed: 23376846]
34. Means AL, Ray KC, Singh AB, Washington MK, Whitehead RH, Harris RC Jr, et al. Overexpression of heparin-binding EGF-like growth factor in mouse pancreas results in fibrosis and epithelial metaplasia. Gastroenterology. 2003; 124:1020–1036. [PubMed: 12671899]
35. Navas C, Hernandez-Porras I, Schuhmacher AJ, Sibilia M, Guerra C, Barbacid M. EGF receptor signaling is essential for k-ras oncogene-driven pancreatic ductal adenocarcinoma. Cancer Cell. 2012; 22:318–330. [PubMed: 22975375]
36. Kroening PR, Barnes TW, Pease L, Limper A, Kita H, Vassallo R. Cigarette smoke-induced oxidative stress suppresses generation of dendritic cell IL-12 and IL-23 through ERK-dependent pathways. J Immunol. 2008; 181:1536–1547. [PubMed: 18606709]
37. Zhang S, Petro TM. The effect of nicotine on murine CD4 T cell responses. Int J Immunopharmacol. 1996; 18:467–478. [PubMed: 9023586]
38. Clark CE, Hingorani SR, Mick R, Combs C, Tuveson DA, Vonderheide RH. Dynamics of the immune reaction to pancreatic cancer from inception to invasion. Cancer Res. 2007; 67:9518–9527. [PubMed: 17909062]
39. Colby JK, Klein RD, McArthur MJ, Conti CJ, Kiguchi K, Kawamoto T, et al. Progressive metaplastic and dysplastic changes in mouse pancreas induced by cyclooxygenase-2 overexpression. Neoplasia. 2008; 10:782–796. [PubMed: 18670639]
40. Bayne LJ, Beatty GL, Jhala N, Clark CE, Rhim AD, Stanger BZ, et al. Tumor-derived granulocyte-macrophage colony-stimulating factor regulates myeloid inflammation and T cell immunity in pancreatic cancer. Cancer Cell. 2012; 21:822–835. [PubMed: 22698406]
41. Pylayeva-Gupta Y, Lee KE, Hajdu CH, Miller G, Bar-Sagi D. Oncogenic Kras-induced GM-CSF production promotes the development of pancreatic neoplasia. Cancer Cell. 2012; 21:836–847. [PubMed: 22698407]
42. Breitman TR, Collins SJ, Keene BR. Terminal differentiation of human promyelocytic leukemic cells in primary culture in response to retinoic acid. Blood. 1981; 57:1000–1004. [PubMed: 6939451]
43. van Bockstaele DR, Lenjou M, Snoeck HW, Lardon F, Stryckmans P, Peetermans ME. Direct effects of 13-cis and all-trans retinoic acid on normal bone marrow (BM) progenitors: comparative study on BM mononuclear cells and on isolated CD34+ BM cells. Ann Hematol. 1993; 66:61–66. [PubMed: 7680579]
44. Kuwata T, Wang IM, Tamura T, Ponnamperuma RM, Levine R, Holmes KL, et al. Vitamin A deficiency in mice causes a systemic expansion of myeloid cells. Blood. 2000; 95:3349–3356. [PubMed: 10828015]
45. Froeling FE, Feig C, Chelala C, Dobson R, Mein CE, Tuveson DA, et al. Retinoic acid-induced pancreatic stellate cell quiescence reduces paracrine Wnt-beta-catenin signaling to slow tumor progression. Gastroenterology. 2011; 141:1486–1497. [PubMed: 21704588]
46. van Geenen EJ, Smits MM, Schreuder TC, van der Peet DL, Bloemena E, Mulder CJ. Smoking is related to pancreatic fibrosis in humans. Am J Gastroenterol. 2011; 106:1161–1166. [PubMed: 21577244]
47. Mohty M, Morbelli S, Isnardon D, Sainty D, Arnoulet C, Gaugler B, et al. All-trans retinoic acid skews monocyte differentiation into interleukin-12-secreting dendritic-like cells. Br J Haematol. 2003; 122:829–836. [PubMed: 12930397]

48. Goswami S, Sahai E, Wyckoff JB, Cammer M, Cox D, Pixley FJ, et al. Macrophages promote the invasion of breast carcinoma cells via a colony-stimulating factor-1/epidermal growth factor paracrine loop. Cancer Res. 2005; 65:5278–5283. [PubMed: 15958574]

49. Edwards JP, Zhang X, Frauwirth KA, Mosser DM. Biochemical and functional characterization of three activated macrophage populations. J Leukoc Biol. 2006; 80:1298–1307. [PubMed: 16905575]

50. Moniaux N, Chakraborty S, Yalniz M, Gonzalez J, Shostrom VK, Standop J, et al. Early diagnosis of pancreatic cancer: neutrophil gelatinase-associated lipocalin as a marker of pancreatic intraepithelial neoplasia. Br J Cancer. 2008; 98:1540–1547. [PubMed: 18392050]

51. Singh AP, Moniaux N, Chauhan SC, Meza JL, Batra SK. Inhibition of MUC4 expression suppresses pancreatic tumor cell growth and metastasis. Cancer Res. 2004; 64:622–630. [PubMed: 14744777]

52. Momi N, Ponnusamy MP, Kaur S, Rachagani S, Kunigal SS, Chellappan S, et al. Nicotine/cigarette smoke promotes metastasis of pancreatic cancer through alpha7nAChR-mediated MUC4 upregulation. Oncogene. 2013; 32:1384–1395. [PubMed: 22614008]

53. Mathison A, Liebl A, Bharucha J, Mukhopadhyay D, Lomberk G, Shah V, et al. Pancreatic stellate cell models for transcriptional studies of desmoplasia-associated genes. Pancreatology. 2010; 10:505–516. [PubMed: 20847583]

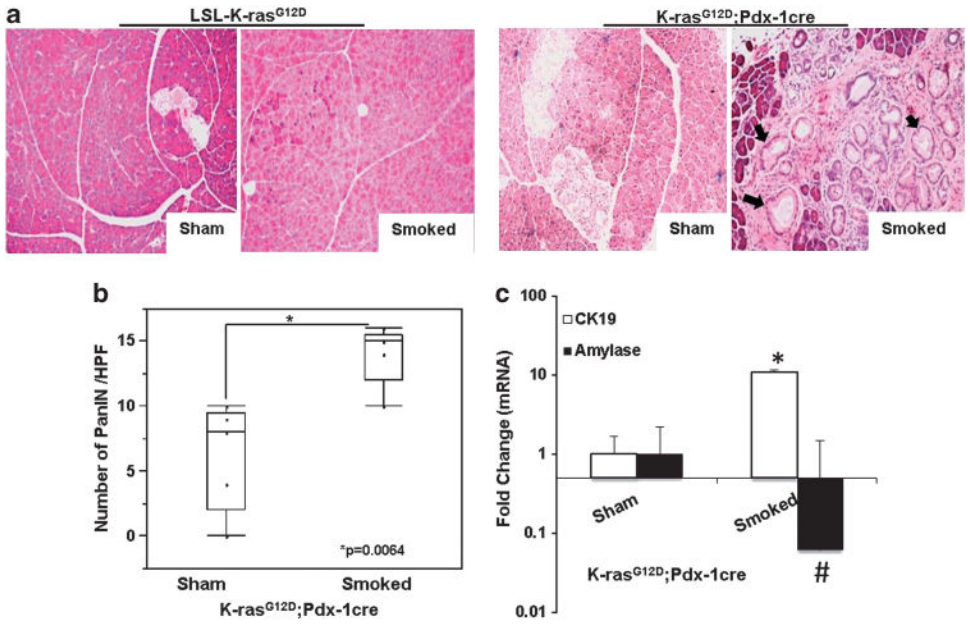

Figure 1.

Smoking accelerates PanIN formation in the spontaneous PC mouse model. (**a**) Hematoxylin and eosin staining of sham and smoke-exposed unfloxed and floxed animals demonstrating the formation of pre-cancerous lesions (PanIN, black arrow) in the floxed mice at 30 weeks of age (magnification × 100). (**b**) Quantification of the number of PanIN lesions (low and high grade) in the sham and smoke-exposed floxed animals. There was a significant increase (P = 0.006) in the number of the PanIN lesions per high-power field (HPF) after smoke exposure. (**c**) Real time reverse transcription PCR analysis of the RNA isolated from the pancreas of sham and smoke-exposed floxed (n =6) animals. There was tenfold increase in the expression of ductal marker CK19 (*P<0.05) and a concurrent decrease in the expression of acinar marker amylase (#P<0.05) after 20 weeks of smoke exposure.

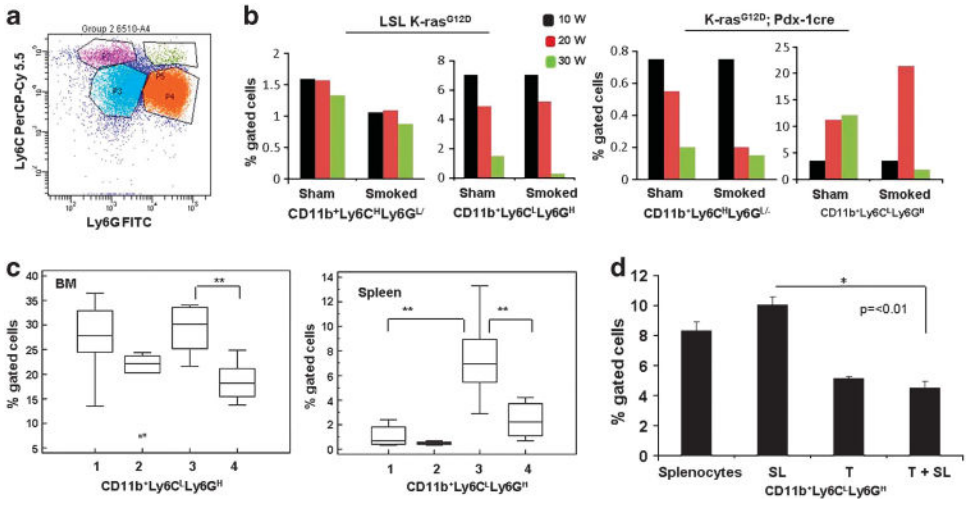

Figure 2.

Smoking decreases the accumulation of MDSCs in the spontaneous PC mouse model. (**a**) Gating strategy for the analysis of different subsets of MDSCs. The granulocytic fraction was identified by the expression of $CD11b^+$ $Ly6C^L$ $Ly6G^H$ (P4) and the monocytic fraction (P2) expresses $CD11b^+$ $Ly6C^H$ $Ly6G^{L/-}$. (**b**) Analysis of different subsets of MDSCs in the peripheral circulation. Blood from six animals from each group were collected by retro-orbital puncture, pooled and analyzed. The samples were drawn at the start of smoking (10 weeks), at the midpoint of smoking (20 weeks) and at the termination of the experiment (30 weeks). There was a significant decrease in granulocytic population after smoke exposure in floxed mice. (**c**) Expansion and accumulation of a subset of MDSCs (granulocytic) in the bone marrow and spleen of animals in various experimental groups. ((1) Unfloxed sham, (2) unfloxed smoked, (3) floxed sham and (4) floxed smoked animals) after 20 weeks of smoke exposure (**P<0.001). There was a significant decrease in the granulocytic subset of MDSCs after the smoke exposure. (**d**) The splenocytes isolated from the 30-week-old floxed mice were treated *in vitro* with the SL and the condition media from untreated (T) or SL-treated tumor cell line KCT 961 (T+SL). There was a significant decrease (*P<0.01) in the percentage of granulocytic fraction after treatment with conditioned media.

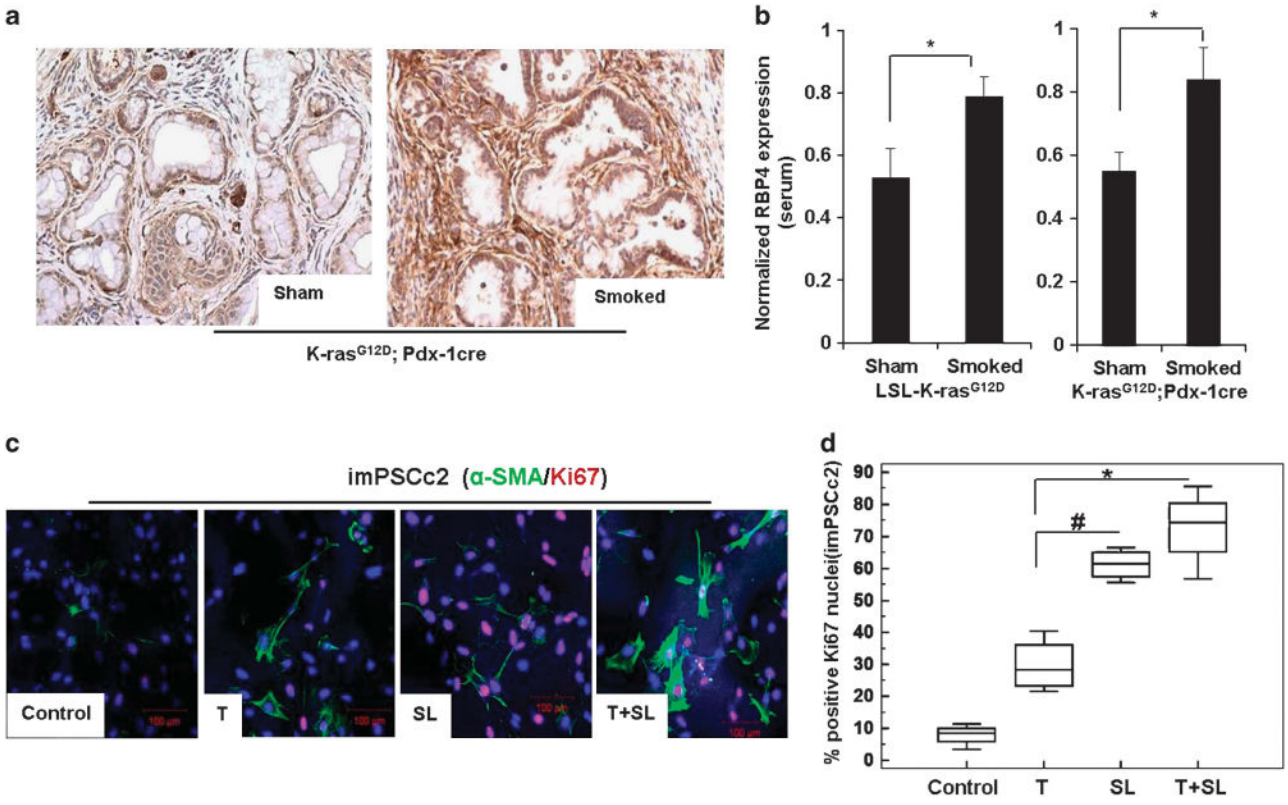

Figure 3.

Smoking induces the activation of PSCs. (**a**) α-SMA (myofibroblast marker) staining in the smoke-exposed and sham control floxed mice. There was higher expression of α-SMA in the pancreas of smoke-exposed animals compared with the sham group, reflecting greater activation status of stellate cells (magnification × 400). (**b**) The normalized levels of retinoic acid-binding protein 4 from the serum of sham (n = 4) and smoke-exposed (n = 4) unfloxed and floxed mice. The smoke-exposed mice showed significantly higher levels of retinoic acid-binding protein 4 (*P<0.05) in the serum, reflecting increased levels of the circulating ATRA. (**c**) Immunofluorescence analysis of the PSCs (imPSCc2) for the expression of α-SMA and Ki-67 after treatment with SL and conditioned media derived from untreated tumor cells (KCT 961, T) and SL-treated tumor cell line (KCT 961, T+SL). There was higher activation and proliferation of PSCs after treatment with SL, T and T+SL. (**d**) Percentage positive Ki-67 nuclei in imPSCc2 cell line after treatment with SL, T and T+SL. The significant increase in the Ki-67 nuclei after treatment with SL (#P<0.001) and conditioned media from SL-treated KCT 961 cell line (*P<0.001) indicated the higher activation and proliferative status of PSCs.

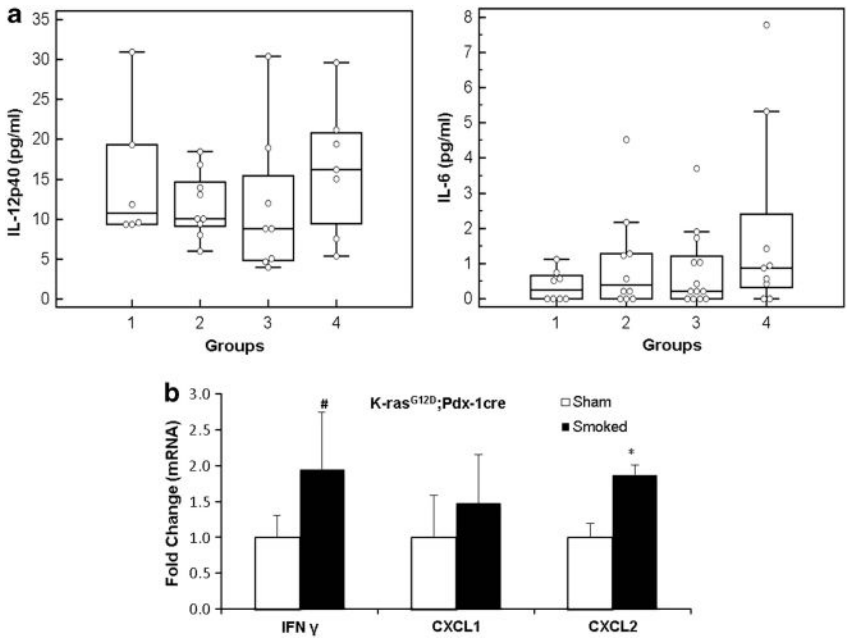

Figure 4.

Smoking-induced changes in the inflammatory cytokines responsible for MDSCs maturation. (a) The box plot comparing the levels of indicated cytokines between four experimental groups: (1) unfloxed sham, (2) unfloxed smoked, (3) floxed sham and (4) floxed smoked. Analyses of the 13 cytokines known to modulate the mobilization, activation and differentiation of cells of myeloid origin were performed from serum samples using the Luminex-based Procarta Cytokine Assay Kit (Supplementary Figure 2). There was an increase in the levels of IL-12p40 and IL-6 after smoke exposure in the floxed animals. (**b**) Real time reverse transcription PCR analysis of inflammatory markers (*IFN-γ*, CXCL1 and CXCL2) in pancreas of floxed mice (sham and smoke exposed). Smoking leads to significant increase in *IFN-γ* ($^{\#}P<0.05$) and CXCL2 ($^{*}P<0.05$) levels in the pancreas compared with sham control, indicating higher inflammatory status in pancreas after smoke exposure.

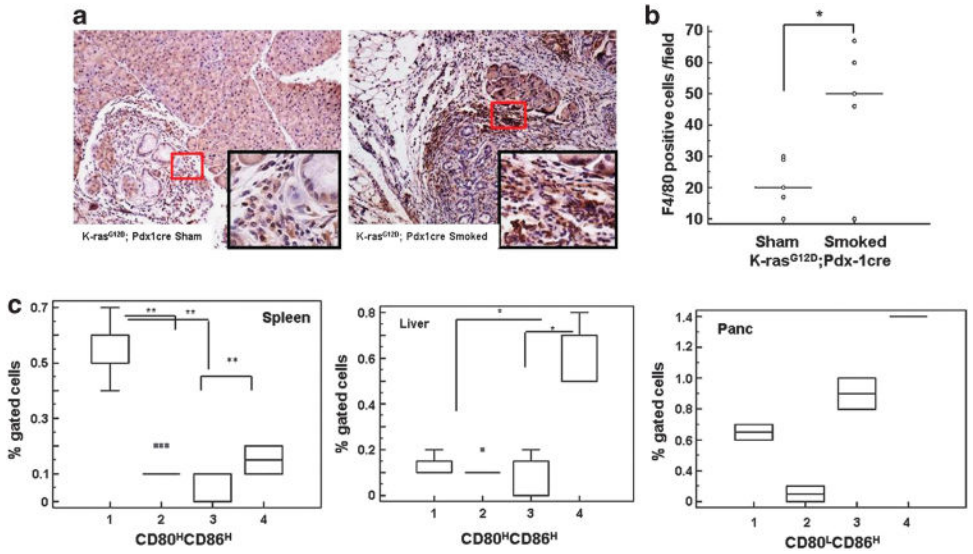

Figure 5.

Increased DC and macrophage accumulation in response to smoking. (**a**) Immunohistochemistry analysis of TAMs (identified by F4/80 staining) in K-ras^{G12D}; Pdx-1cre smoke-exposed animals compared with the sham control (magnification × 100; inset × 400). (**b**) Quantification of TAMs from sham and smoke-exposed animals showed significant increase in TAMs in the pre-neoplastic lesions in the pancreas (**P*<0.05) after smoke exposure (average count of F4/80-positive cells in five independent fields/tissue section). (**c**) Analysis of the distribution of DCs in spleen, liver and pancreas in (1) unfloxed sham, (2) unfloxed smoked, (3) floxed sham and (4) floxed smoked animals. There was significantly higher DC population in the spleen and liver as defined by CD80/CD86 positivity after smoke exposure in floxed mice compared with sham (**P*<0.05, ***P*<0.001).

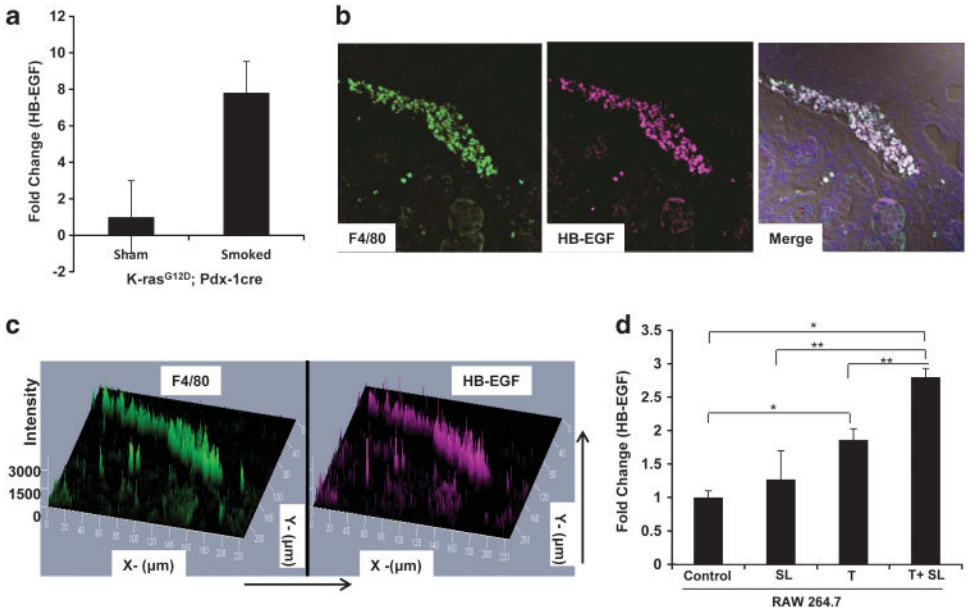

Figure 6.

Smoking induces the expression of HB-EGF in the macrophages. (**a**) Real time reverse transcription PCR analysis of the expression of HB-EGF in the pancreas of the sham and smoke-exposed floxed mice. There was higher expression of HB-EGF in the pancreas in response to smoking. (**b**) Immunofluorescence analysis of the pancreas of smoke-exposed floxed mice stained with macrophage marker (F4/80) and the HB-EGF antibodies. Macrophage population was the predominant source of the HB-EGF in PanIN lesions as demonstrated by intensity plot of colocalization of F4/80 and HB-EGF. (**c** and **d**) The in vitro treatment of mouse macrophage cell line RAW 264.7 with SL and conditioned media derived from untreated tumor cells (KCT961, T) and SL-treated tumor cell line (KCT961, T +SL) showed a significant increase of 2.8-folds in HB-EGF at transcription level (*P<0.01, **P<0.05).

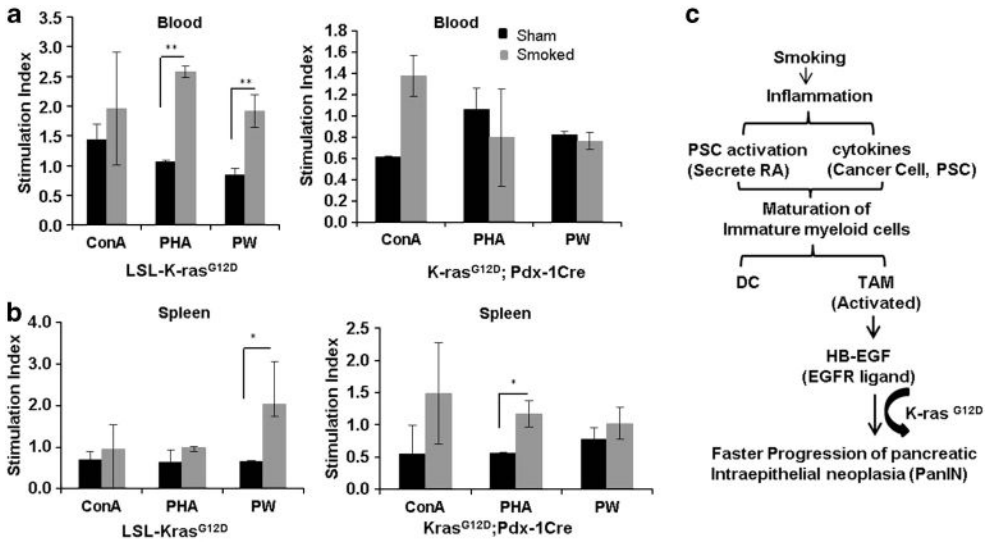

Figure 7.

Smoking partially suppresses the immune system during early stages of PC. (a) Mitogen stimulation (Con A, PHA and PW) of peripheral blood mononucleated cells derived from sham and smoke-exposed unfloxed and floxed animals. The lymphocytes from smoke-exposed unfloxed mice proliferated at significantly higher rate (**P = 0.0005) compared with sham control, which was reduced in the floxed mice after smoke exposure. (**b**) Mitogen stimulation (Con A, PHA and PW) of splenocytes derived from sham and smoke-exposed unfloxed and floxed mice. There was no effect on the mitogenic potential of the splenocytes after smoke exposure. (**c**) Proposed model of the cigarette smoke-induced acceleration of the PC. Smoking induces the inflammation that leads to the activation of the PSCs and changes the cytokine profile, which results in the maturation of the immature cells of the myeloid origin to macrophages and DCs. Smoking further induces the expression of EGFR ligands (HB-EGF) in the macrophages, which in conjunction with the mutant K-ras accelerates the progression of PC.